COMPARISON OF 3D INTEGRATED GEOPHYSICAL MODELING IN THE SOUTH CAUCASIAN AND EASTERN MEDITERRANEAN SEGMENTS OF THE ALPINE-HIMALAYAN TECTONIC BELT

L.Eppelbaum

Tel Aviv University,
Ramat Aviv 69978, Tel Aviv, Israel

South Caucasus (including Azerbaijan) and Easternmost Mediterranean (including Israel) are located within the Alpine-Himalayan tectonic belt and are characterized by complex and variable tectono-geological pattern. To study deep structure of these regions several regional interpreting profiles indicating results of 3D combined gravity-magnetic modeling were selected. Development of the initial physical-geological models (***PGM***s) is realized by utilization of the known surface geology, drilling data examination, previous seismic, magnetotelluric and thermal data analysis, careful investigation of the petrophysical (including paleomagnetic) data, as well as qualitative and quantitative analysis of gravity-magnetic materials. After that an iterative 3D modeling accompanied by changing geometrical boundaries of geological bodies (and assuming new targets) and varying physical properties (density, magnetization and magnetic vector inclination) is started. This process has been completed by development of final ***PGM***s. Creating the final ***PGM***s means not only determination of minimal difference between the observed and computed gravity and magnetic fields, but also compliance of the models with the known geological principles (complex geological ***PGMs*** of the regions under study often compose intricate structural-tectonic puzzles). The final ***PGM***s reflect the key structural-tectonic specifics of the regional geological structure, beginning from the subsurface (hundreds of meters) up to the Moho discontinuity (tens of kilometers). The ***PGM***s revealed primarily the boundaries of tectonic blocks, masked faults, buried uplifts of basement, occurrence and form of various magmatic bodies, some common factors controlling ore- and hydrocarbon bearing formations, and some other features. This investigation briefly summarizes the principles and possibilities of advanced 3D combined modeling of gravity and magnetic fields and presents several essential ***PGM***s for the regions under study.

Introduction

The Alpine-Himalayan tectonic belt (AHTB) includes an array of mountain ranges which extends along the southern margin of Eurasia, stretching from islands of Java and Sumatra through the Himalayan Mts., Mediterranean Sea, and out into the Atlantic Ocean, on the total distance of about 16,000 km (Khain, 2000). The AHTB is a typical collision-type orogenic belt formed during tens of million years after the closure of the Mesozoic – Early Cenozoic Tethys Ocean. It is characterized by an intensive mountain building and rifting which were accompanied by extensive plateau basaltic and andesite-latite magmatism (Sharkov et al., 2015).

The South Caucasus and Easternmost Mediterranean are the central segments of this tectonic belt, but their geological structure is strongly differing (see corresponding sections below). Seismic analysis is accepted now as a leading (and expensive) geophysical method for deep structure investigation. However, not in all situations (especially for the areas with the predominant distribution of sub-vertical targets) seismic analysis may provide effective and reliable results. At the same time comprehensive analysis of comparatively inexpensive gravity-magnetic data can not only to significantly extend the seismic data interpretation, but also to obtain data which are not unattainable by the seismic data examination. A 3D combined gravity-magnetic modeling is the most powerful and simultaneously is the most complex interpretation tool of potential geophysical field analysis. Its effective application suggests besides the obvious physical-mathematical basis the good knowledge of geological methods of analysis on the whole and familiarity with a concrete geology of the region under study.

Preferences of integrated interpretation

Gravity-magnetic data processing is generally intended to reduce and eliminate noise factors of different origins and intensities. The main problem faced by qualitative interpretation is to single out a desired target, whereas quantitative interpretation needs to determine and refine the target parameters. Thus, geological problems need to be resolved in terms of: (1) the capabilities of the geophysical method selected for measurements of the field containing the information required, (2) the physical properties of the medium under study and their capability to generate detectable signals (anomalies), (3) the methods for data processing and interpretation; namely, their ability to extract information from geophysical fields and reveal the effects from the geological targets. Figure 1 presents a general flow-chart for analysis and synthesis of geophysical data for complex regions. Each step in this flow-chart is divided into sub-steps with more concrete formulation (Khesin et al., 1996).

Estimation of efficiency of geophysical integration from the probabilistic and information points of view is considered in detail in Eppelbaum (2014b). Interestingly that from analysis of a classical "Four Color Problem" follows that two geophysical method applications theoretically is sufficient for successive mapping of the area of any geological complexity (Eppelbaum, 2014a). Undoubtedly this fact supports the theoretical basement of 3D combined gravity-magnetic field modeling.

Short description of the employed algorithm

The *GSFC* (Geological Space Field Calculation) program was developed for solving a direct 3-D gravity and magnetic prospecting problem under complex geological conditions (Khesin et al., 1996; Eppelbaum and Khesin, 2004). This program has been designed for computing the field of Δg (Bouguer, free-air or observed value anomalies), components of magnetic field ΔZ, ΔX, ΔY, total magnetic field ΔT, as well as second derivatives of the gravitational potential under conditions of rugged relief and inclined magnetization. The geological space can be approximated by (1) three-dimensional, (2) semi-infinite bodies, and (3) those infinite along the strike closed, left hand (LH) non-closed, right hand (RH) non-closed, and open bodies (Figure 2). Geological bodies are approximated by horizontal polygonal prisms with arbitrary number of characteristic points (a simplified example is given in Figure 3).

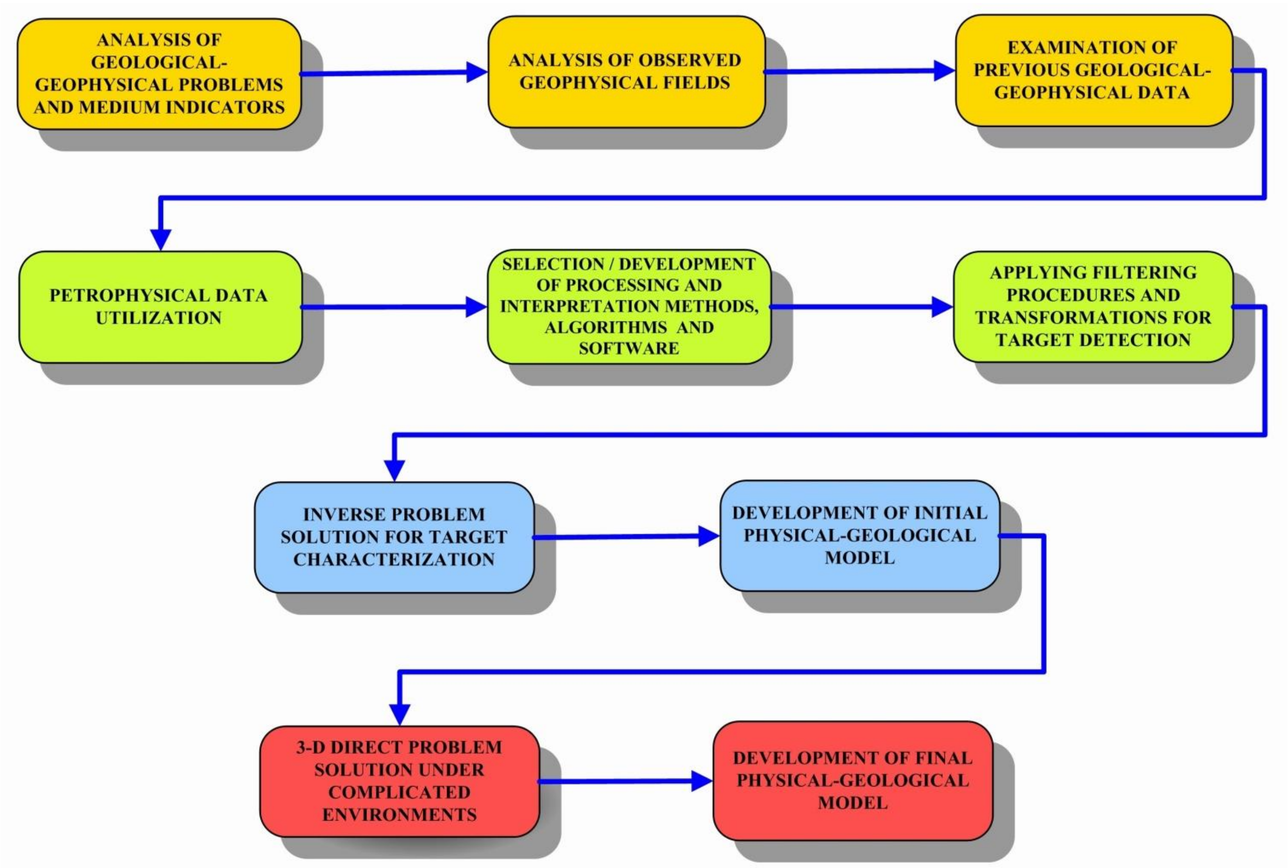

Figure 1. Interpretation of geophysical fields under complex environments: A general scheme

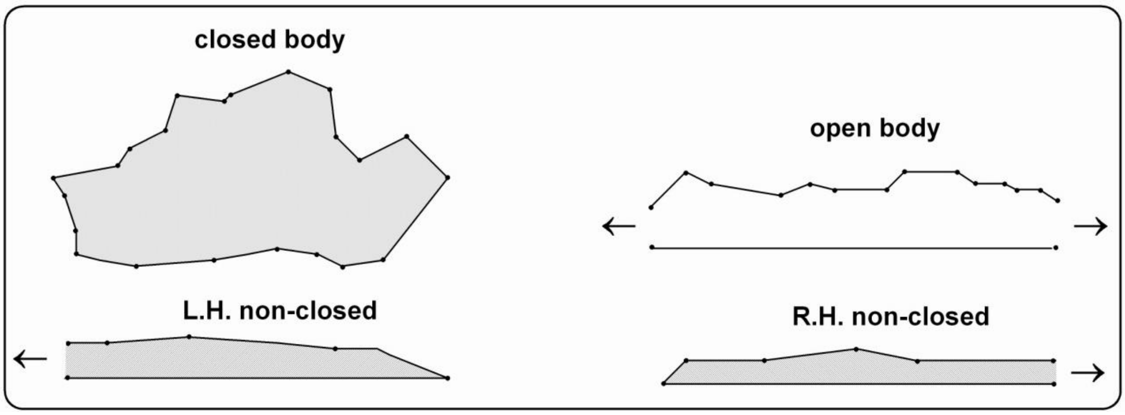

Figure 2. Types of geological bodies used in modeling

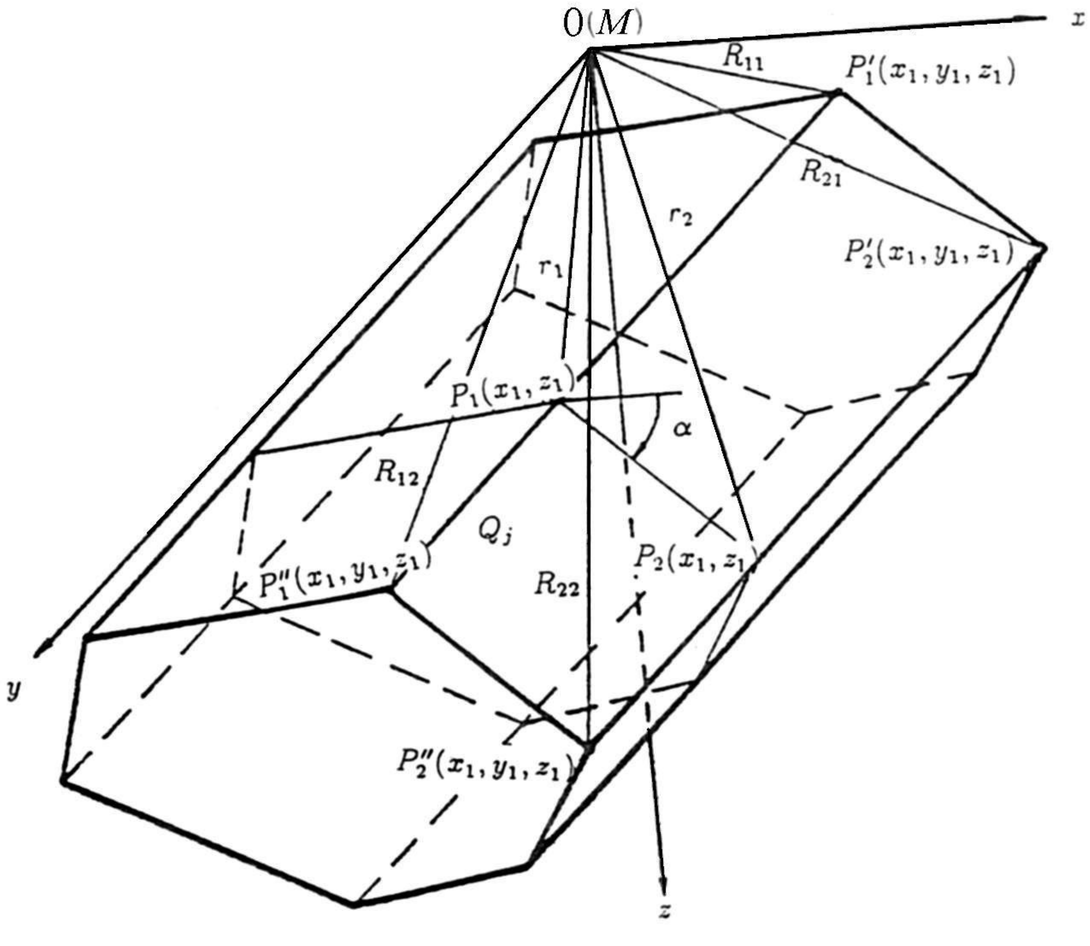

Figure 3. Computing derivatives of gravity potential for a horizontal polygonal prism

The program has the following main advantages (besides above-mentioned ones): (1) Simultaneous computing of gravity and magnetic fields; (2) Description of the terrain relief by irregularly placed characteristic points; (3) Computation of the effect of the earth-air boundary directly in the process of interpretation; (4) Modeling of the interpreting profiles draping over rugged relief or at various arbitrary levels (using characteristic point description); (5) Simultaneous modeling of several profiles; (6) Description of a large number of geological bodies and fragments (up to 1,000). The basic algorithm realized in the GSFC program is the solution of the direct 3-D problem of gravity and magnetic prospecting for the horizontal limited in the strike polygonal prism (Figure 3). In the developed algorithm integration over a volume is realized on the surface limiting the anomalous body.

Analytical expression for the first vertical derivative of gravity potential of (m-1) angle horizontal prism (Figure 3) has been obtained by integrating a common analytical expression:

$$W_{z'} = -\int_s \frac{z}{(R+y)R} dxdz \Big|_{y_1}^{y_2}, \tag{1}$$

where $R = \sqrt{x^2 + y^2 + z^2}$, S is the area of normal section of the prism by the plane of xOz.

$$W_{z'T} = \left\{ \begin{array}{l} -f\sigma \sum_{j=1}^{m-1} \Bigg[V_j \sin\alpha_j \left(\ln \frac{R_{12j}+y_2}{R_{22j}+y_2} - \ln \frac{R_{11j}+y_1}{R_{21j}+y_1} \right) \\ +V_j \cos\alpha_j \left(\operatorname{sgn}(y_2 V_j) \arccos \frac{V_j^2 R_{12j} R_{22j} + U_{1j} U_{2j} y_2^2}{r_{1j} r_{2j} \left(y_2^2 + V_j^2\right)} \right) \\ -\left(\operatorname{sgn}(y_1 V_j) \arccos \frac{V_j^2 R_{11j} R_{21j} + U_{1j} U_{2j} y_1^2}{r_{1j} r_{2j} \left(y_2^2 + V_j^2\right)} \right) \\ +\cos\alpha_j \left(y_2 \ln \frac{R_{12j}+U_{1j}}{R_{22j}+U_{2j}} - y_1 \ln \frac{R_{11j}+U_{1j}}{R_{21j}+U_{2j}} \right) \Bigg] \end{array} \right\}, \tag{2}$$

here f is the gravitational constant, σ is the density of the body and α_j is the angle of the prism's side inclination.

$$\left. \begin{array}{l} \cos\alpha_j = \dfrac{x_{2j} - x_{1j}}{r_{12j}} \\ \sin\alpha_j = \dfrac{z_{2j} - z_{1j}}{r_{12j}} \end{array} \right\}, \tag{3}$$

x_{1j}, z_{1j} and x_{2j}, z_{2j} are coordinates of points P_{1j} and P_{2j} (angle points of j-side of (m-1) polyhedron); r_{12j} is the length of j-side of this polyhedron:

$$r_{12j} = \sqrt{(x_{2j} - x_{1j})^2 + (z_{2j} - z_{1j})^2}, \tag{4}$$

r_{1j} and r_{2j} are distances from the selected point M to the points P_{1j} and P_{2j}, respectively:

$$\left. \begin{array}{l} r_{1j} = \sqrt{x_{1j}^2 + z_{1j}^2} \\ r_{2j} = \sqrt{x_{2j}^2 + z_{2j}^2} \end{array} \right\}, \tag{5}$$

R_{11j}, R_{21j}, R_{12j}, R_{22j} are distances from the selected point M to angle points $R_{1j'}$, $R_{2j'}$, $R_{1j''}$ and $R_{2j''}$, respectively, for j-side of the prism:

$$\left. \begin{array}{l} R_{11j} = \sqrt{r_{1j}^2 + y_1^2} \\ R_{21j} = \sqrt{r_{2j}^2 + y_1^2} \\ R_{12j} = \sqrt{r_{1j}^2 + y_2^2} \\ R_{22j} = \sqrt{r_{2j}^2 + y_2^2} \end{array} \right\}. \tag{6}$$

U_{1j}, U_{2j} and V_j are the visible solid angles of corresponding parts of the prism's j-th side (see Figure 3).

The values of the gravitational and magnetic fields at the selected point M are determined using the following formulas:

$$\Delta g = CMf\sigma U_{z'}, \tag{7}$$

$$\Delta Z = I_z U_{z'z'} + I_x U_{x'z'} + I_y U_{y'z'}, \tag{8}$$

$$\Delta X = I_x U_{x'z'} - I_x \left(U_{z'z'} + U_{y'y'}\right) + I_y U_{x'y'}, \tag{9}$$

$$\Delta Y = I_z U_{y'z'} + I_{x'y'} + I_y U_{y'y'}, \tag{10}$$

$$\begin{array}{l} \Delta T = W_{zz} U_{z'z'} + W_{zx} U_{z'x'} + W_{yy} U_{y'y'} + \\ \quad + W_{yz} U_{y'z'} + W_{xy} U_{x'y'}, \end{array} \tag{11}$$

where CM is the scale of the chart; f = 0.00667 (gravitational constant is given in 10^{-8} SI unit, i.e. measured in 10^{-8} m^3 $kg^{-1}s^{-2}$); σ is the body's excess density determined using the formula:

$$\sigma = \sigma_d - \sigma_s. \tag{12}$$

Here σ_d and σ_s are the densities of the anomalous body and the surrounding medium, respectively. Density is given in 10^3 SI unit (10^3 kg/m^3), i.e. in g/cm^3. At such dimensions of the density and gravitational constant, the computed gravity field will be obtained in 10^{-5} SI unit (10^{-5}m/s^2 = milliGal (mGal)). I_z, I_x and I_y are the components of the excess magnetization vector determined using the following formulas (revised after Khesin et al., 1996):

$$I_z = 0.1\left[I_d \sin J_d - I_s \sin J_s\right], \tag{13}$$

$$I_x = 0.1\left[I_d \cos J_d \cos(A_d - A_x) - I_s \cos J_s \cos(A_s - A_x)\right], \tag{14}$$

$$I_y = 0.1\left[I_d \cos J_d \sin(A_d - A_x) - I_s \cos J_s \sin(A_s - A_x)\right], \tag{15}$$

where I_d and I_s are magnetization values for the anomalous body and the surrounding medium, respectively; the coefficient 0.1 is introduced to obtain the magnetic field plots in nanoTesla (nT); J_d and J_s are the inclinations of the magnetization vector of the body and the medium to the horizon, respectively; A_d and A_s are azimuths of the magnetization vector horizontal projections for the anomalous body and the medium, respectively; A_x is the azimuth of the interpreting profile. Detailed description of analytical expressions for the first and second derivatives of gravity potential of the approximation model of the horizontal polygonal prism and their connection with magnetic field is presented in Khesin et al. (1996) and Eppelbaum et al. (2000).

Let us discuss shortly the constantly arisen problem of development of an automatic system of 3D combined gravity-magnetic field modeling. Suppose we conduct 3-D integrated gravity and magnetic modeling over a geological section consisting of ten geological bodies. Each geological body has three petrophysical variables (density, value and inclination of the magnetization vector), and geometric variables: geometric parameters in the plane of geological section (x_i, z_i), left-hand (y_{i1}) and right-hand (y_{i2}) end faces of each body. Number of points (variables) necessary for describing bodies in the plane of section *a priori* is unknown. For simplicity and taking into account that many of these points are calculated two times by contouring objects, we can assume that the number of these points is ten. To calculate the possible number of combinations of all variables by the integrated 3-D modeling, we should carry out approximated ranging of variables (Table 1). Undoubtedly, this ranging is relative and is executed only for an estimation of necessary order number of combinations.

Applying known combinatorial analysis (e.g., Riordan, 2014), for one body we have the number of combinations $C_{30}^1 \cdot C_{60}^1 \cdot C_{24}^1 \cdot C_{30}^1 \cdot C_{30}^1 \cdot C_{100}^1 \approx 4 \cdot 10^9$. Correspondingly, for ten bodies we have $\approx 4 \cdot 10^{90}$ combinations. Obviously, such a number of combinations considerably complicates an automatic 3-D integrated gravity-magnetic modeling even using supercomputers.

Description of interpretation methodology

The most complete description of the interpretative process structure was given by Strakhov (1976). An interpretation process may be roughly subdivided into the following stages: (1) summarizing prior information; (2) sequential analysis, and (3) geological synthesis.

The development of 3-D ***PGM*** is usually performed using these three stages.

The first stage (summarizing prior information) is as follows:

(A) First of all the main geological-geophysical conception of tectonic development of the region under study must be analyzed and adopted (without it the process of *PGM* construction will be not successive and logical). Construction of geological section includes compilation of all intrusive, effusive and other associations, as well as faults and the surface of folded foundation on the basis of geological data within a strip of 15-20 km (in some cases – 20-40 km) wide. The interpreting section is located in the middle of this strip. Undoubtedly, geophysicist-interpreter must have a good knowledge of the region under study.

Such a section characterizes the upper portion of the Earth's crust with a thickness from 2-3 to 5-8 km from the Earth's surface to the Baikalian (this complex is termed as Cadomian in western publications (Khain, 2007)) basement. Deeper parts of the intrusive bodies and certain faults are formed by extrapolation of the available constructions, general geological considerations and the results of previous geophysical analyses.

Table 1

Calculation of the number of possible combinations of variables

Variable	Interval of changing	Ranging	Number of combinations
Density, g/cm^3	2.30-2.60	0.01	30
Magnetization, mA/m	0-3000	50	60
Inclination of magnetization, degree	0-360	15	24
Left-hand end face, y_1/x_m*	0-20	non-linear	30
Right-hand end face, y_2/x_m	0-20	non-linear	30
Geometrical coordinates of geological body in the plane of geological section	min 10 points	–	min 10·10

*x_m is the maximum length of interpreting profile.

(**B**) A preliminary petrophysical model of the section is developed. Here all the geological bodies acquire density and magnetization values according to the preceding petrophysical data analysis and results of geophysical field interpretation. When no data are available on the magnetization direction, it is assumed to be parallel to the normal geomagnetic field in the region under study. Further, the magnetization direction is refined in the process of physical-geological modeling. Density properties are received from the borehole sample examination and converted from the seismic data by the known method (e.g., Barton, 1986). The petrophysical model includes deep-seated layers (slabs) of the Earth's crust: (1) the "basaltic", (2) the intermediate between the crust and the upper mantle, and (3) the upper mantle. Their surfaces are constructed and physical properties are associated with them according to the data from previous seismic, magnetotelluric, thermal and other geophysical studies. Paleomagnetic data examination may be of a high significance (it is shown below on example of the Easternmost Mediterranean).

(**C**) The initial (preliminary) petrophysical model includes hidden bodies as well. Their location, thickness, depth, density and magnetization are obtained from the quantitative analysis of magnetic and gravity fields as well as from seismic data examination.

The second stage (sequential analysis) includes application of combined gravity and magnetic field modeling along the interpreting profiles using 3D *GSFC* program (sometimes other software – EMIGMA – was applied). Each time the gravity-magnetic effects from different bodies, groups of bodies and the total computed model are displayed and compared to the observed gravity and magnetic fields. Using the results of this comparison, the changes that match the gravity and magnetic effects into the model of the medium are introduced. The computations and comparisons of fields and model modifications are repeated until the desired fit between the computed and observed fields is obtained.

Then, a regional gravity (and sometimes magnetic) field is roughly selected. As a rule, the densities of deep-seated complexes are not changed; the modifications only affect the shape of their roof. Next, geophysical fields of local bodies are selected. If necessary, this is followed by a verification of the regional fields and the fields of the local bodies.

At each computational step, a separate analysis of gravity and magnetic fields is carried out. Geometrical coordinates of geological bodies are verified in the subsequent steps, and then introduced into the model. This procedure leads to an integrated qualitative and quantitative interpretation for anomalous gravity and magnetic fields. The modeling completes when the computed gravity and magnetic fields coincide accurately with the observed fields. All this modeling process must be carried out in a full compliance with the known geological principles.

The third stage (geological synthesis) involves a detailed geological interpretation of these models. A 3-D ***PGM*** of the area under investigation is developed based on the geological data obtained at the previous stages and qualitative and quantitative geophysical data examination. This yields the final physical-geological sections, and the models are characterized by a more complete rendering of the geological targets, including crustal blocks, intrusions, faults, and economic deposits.

The geological interpretation of the geological associations, complexes and local bodies of the constructed (final) petrophysical model does usually not consist of a hard problem since in the implementation of the interactive selection system almost all the bodies in the ***PGM*** acquire some specific geological content. The geological nature of new sources introduced into the model during the iterative modeling and reflected either in the initial geological section, or in the initial ***PGM***, is determined according to the similarity of their physical properties, dimensions, and depth of occurrence with respect to the known targets. The age of the bodies is determined according to their interrelations with the surrounding (host) rocks.

Application of 3D combined modeling of gravity-magnetic fields in the South Caucasus and Eastern Mediterranean

South Caucasian segment of the Alpine-Himalayan tectonic belt

Brief geological-geophysical background

The complexity of Azerbaijan's territory geological structure stems from its location in the AHTB (e.g., Khain and Alizadeh, 2005; Leonov, 2008). The NE part of Azerbaijan is a fragment of the Pre-Caucasian foreland filled by Cenozoic terrigenous sediments. A heterogenic Nakhichevan folding system is located in the SW part, where carbonate Paleozoic strata and Cenozoic magmatic formations are mixed (Figure 4). At the mega-anticlinorium of the Greater Caucasus, stratified Cenozoic and Mesozoic thick (predominantly, sedimentary) strata are presented. The prevalence of Mesozoic magmatic formations is typical of the mega-anticlinorium of the Lesser Caucasus. The Kura mega-synclinorium, dividing the Greater and Lesser Caucasus, is characterized by an accumulation of thick (up to several kilometers) Cenozoic terrigenous sediments. The Talysh anticlinorium is located on the SE flank of the Kura depression, where Paleogene magmatic associations are widely distributed (Khain and Alizadeh, 2005).

According to Khain (2000), the most ancient Pre-Baikalian structural complex is characterized by a sub-meridional strike. A less metamorphosed Baikalian complex is rumpled to latitudinal folds in separate areas. The Caledonian complex is practically unknown. The Hercynian complex is characterized by a Caucasian strike identical to the overlying Mesozoic rocks.

The Alpine tectono-magmatic cycle is characterized by more complete geological data. As a whole, for Azerbaijan territory is typical the frequently changing geological associations on the vertical and lateral axes, the presence of multifarious fold and fault structures of different orders, and regional and local metamorphism (Alizadeh, 2012). All these factors make the development of reliable models of these media sufficiently complex.

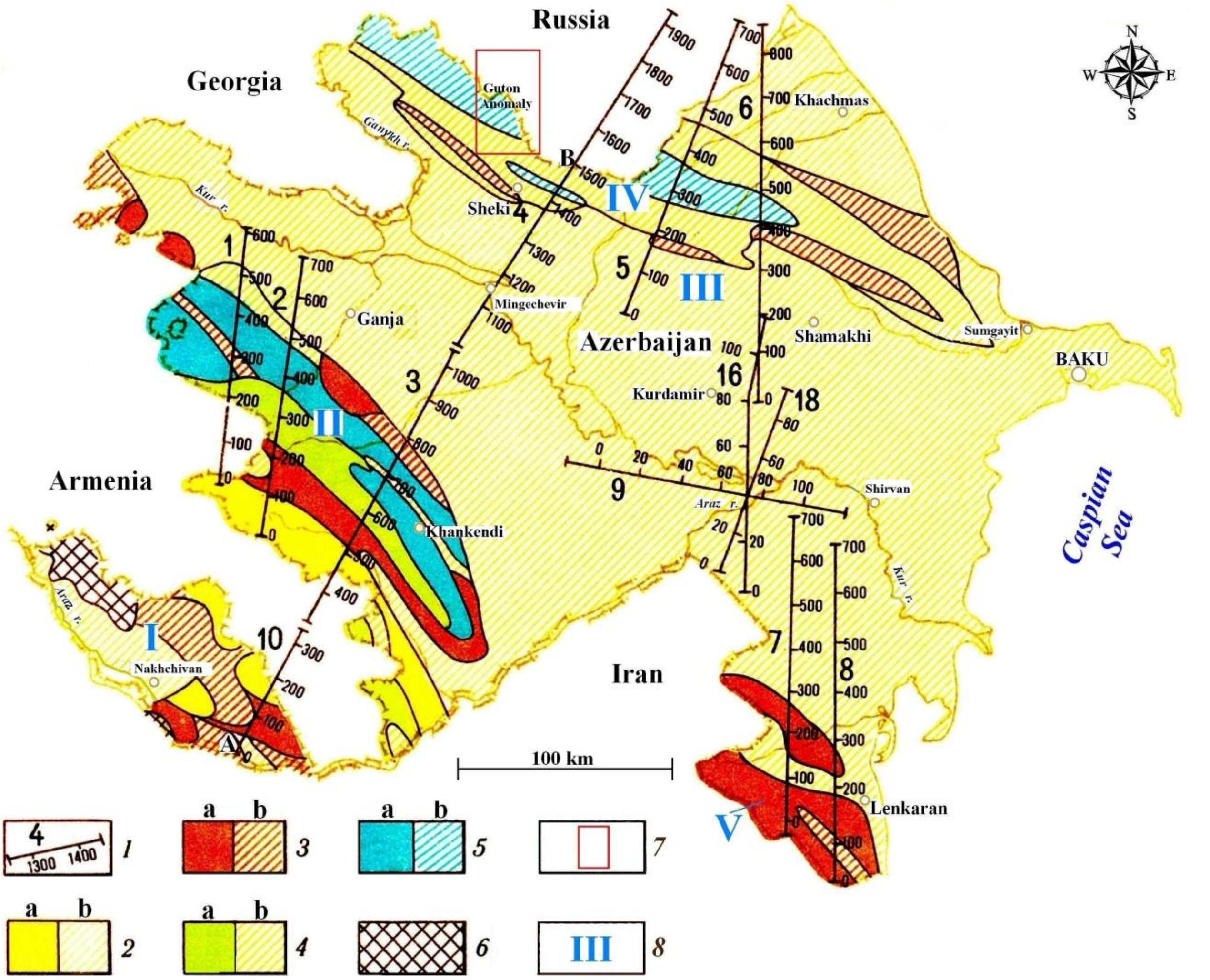

Figure 4. Areal map of some profiles used for physical-geological modeling in Azerbaijan and adjacent regions
(1) profiles and pickets, (2) Pg_3-Q: (a) orogenic magmatic associations, (b) background sedimentary deposits, (3) K_2-Pg_2: (a) pre-orogenic magmatic associations, (b) background sedimentary deposits, (4) J_3-K_1: (a) magmatic associations of the Late Alpine sub-stage, (b) background sedimentary deposits, (5) J_1-J_2: (a) magmatic associations of the Early Alpine sub-stage, (b) background sedimentary deposits; (6) *Pz* deposits, (7) contour of the Guton magnetic anomaly, (8) tectonic regions: I – Nakhchivan folding region, II – SE part of the Lesser Caucasus mega-anticlinorium, III – central and SE parts of the Kura mega-synclinorium, IV – SE part of the Greater Caucasus mega-anticlinorium, V – Talysh anticlinorium

The first models of the Earth's crust of Azerbaijan were put forward in the mid-1960s (Gadjiev, 1965; Tzimelzon, 1965; Shekinsky et al., 1967). These models were subsequently evaluated in the works of Tzimelzon (1970), Azizbekov et al. (1972), Shikhalibeyli (1972), Alexeyev et al. (1988), and later by Khesin et al. (1993, 1996). Rappel and McNutt (1990) studied the regional compensation of the Greater Caucasus using the Bouguer gravity. Sarker and Abers (1998) attempted to apply *P* and *S* wave tomography for examination of the Greater Caucasus deep structure. After that new models developed on the basis of gravity field analysis were presented in Kadirov (2000).

Some significant regional peculiarities of the deep structure of the South Caucasus were reflected in: Alexidze et al. (1993), Pilchin and Eppelbaum (1997), Artyushkov et al. (2000), Gasanov (2001), Kaban (2002), Brunet et al. (2003), Guliyev and Panachi (2004), Alizadeh (2005), Khain and Alizadeh (2005), Allen et al. (2006), Kadirov (2006), Khalafly (2006), Reilinger et al. (2006), Saintot et al. (2006), Spichak (2006), Gamkrelidze and Shengelia (2007), Khain (2007), Leonov (2008), Ricketts et al. (2008), Mamedov (2009), Mosar et al. (2010), Eppelbaum and Khesin (2012), Koulakov et al. (2012), Etirmishli and Kazimova (2013), Forte et al. (2013), Mederer et al. (2013), Ruban (2013), Mumladze et al. (2015). and others. In their recent publication Kadirov and Gadirov (2014) demonstrated an effective gravity field modeling along profiles crossing the South Caspian Basin.

Thus, it was recognized that 3D gravity-magnetic modeling is a powerful tool for studying the variable deep structure of the South Caucasus. This study must be preceded by a combined qualitative and advanced quantitative gravity/magnetic data analysis supported by integrated examination of available geological, seismic, magnetotelluric and thermal data, and utilization of numerous magnetic, paleomagnetic and density properties of geological samples from the region under study. Final product of such an investigation is development of series of 2.5 and 3D ***PGM***s. These ***PGM***s can be used not only for substantiation of various types of prospective economic deposits, but also to delineation of the tectonic-structural factors affecting the long-term seismological prognosis (Eppelbaum and Khesin, 2012).

Results of 3D combined gravity-magnetic modeling

Advanced interpretation methods (improved modifications of tangents, characteristic point methods and areal method) were applied to study gravity and magnetic anomalies along all profiles surrounding SuperDeep borehole SD-1 in Saatly area of Azerbaijan. A fragment of this interpretation along Profile 18 is shown in Figure 5. First of all, note that the behavior of the magnetic ΔZ curve and graph $\partial \Delta g_B / \partial x$ are very simular, which testifies to the fact that these anomalies are due to the same geological objects. A quantitative analysis of the magnetic curve allowed to delineate two magnetic targets. The main target apparently is a source of the Talysh-Vandam gravity anomaly (its upper edge coincides with the data obtained by SD-1 drilling) (Khain and Alizadeh, 2005). The obtained data were utilized by construction of a ***PGM*** of first approximation for 3D combined physical-geological modeling (Eppelbaum and Khesin, 2012).

A visual example of 3D combined modeling of gravity and magnetic fields along Profile 1 (see scheme of profiles presented in Figure 4) is shown in Figure 6. Profile 1 crossing the Lesser Caucasus illustrates the very complex geological structure of this region. The Late-Alpine effusives in the ***PGM***s compose an ophiolite zone (relic of the ocean crust). It is thought that the same rocks occur in the NE immersion of the Lesser Caucasus. Pre-orogenic and orogenic intrusive and effusive rocks are fixed in the southern parts of the ***PGM***. Thick sedimentary deposits are developed in northern part of this profile. A smooth high of the Moho discontinuity is observed from south to north from a depth of 52 km up to 42 km (Eppelbaum and Khesin, 2012). Such a Moho boundary behavior on the whole agrees with the latest data of deep seismic profile re-interpretation (Pavlenkova, 2012). Depths of the magnetized bodies lower edges were estimated on the basis of various geophysical field analyses (Pilchin and Eppelbaum, 1997). Here were revealed such classes of disturbing objects as acid intrusions of lower density and magnetization, basic magmatic rocks of increased density and magnetization, and fault zones. It was determined that the clearest density boundaries were associated with the base of the Cenozoic sedimentary strata and, to a lesser degree, with the base of the Alpine complexes. According to the performed modeling geomagnetic boundaries are associated mainly with the roof and bottom of the Mesozoic floor of heightened magnetization.

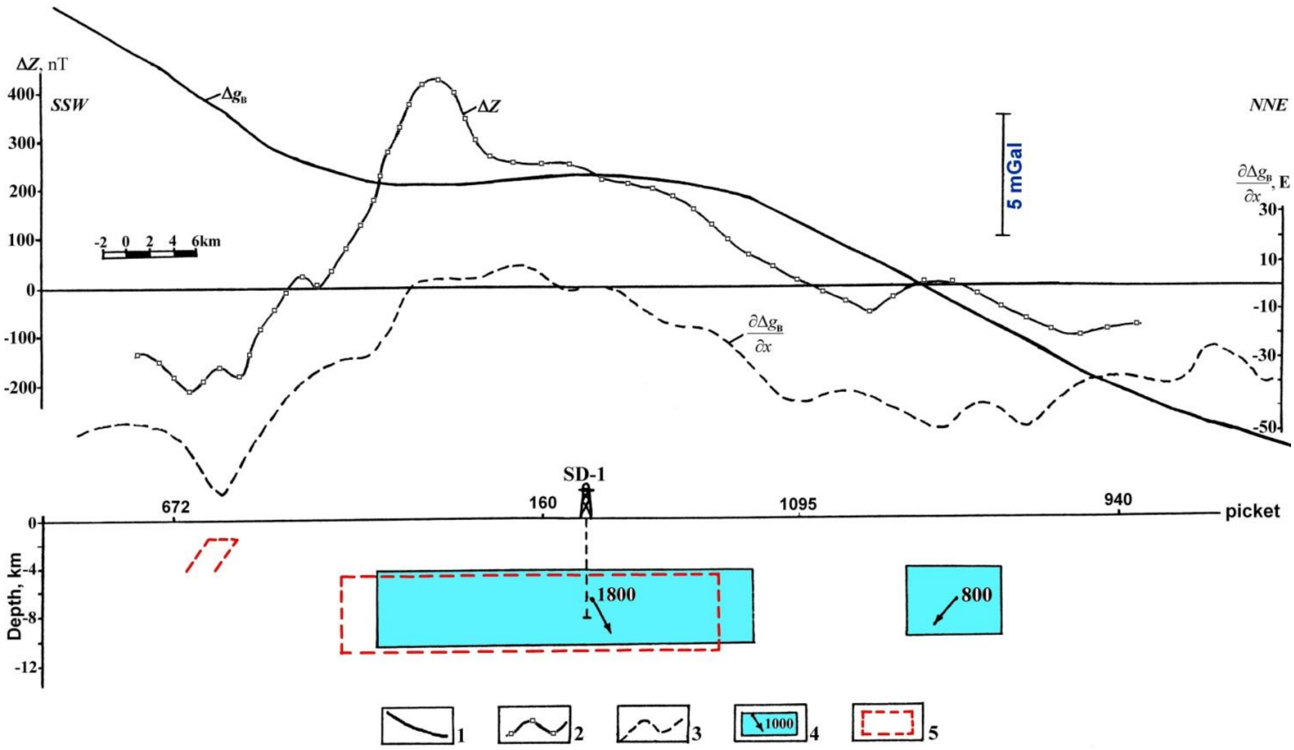

Figure 5. Fragment of gravity and magnetic field analysis along profile 18 (location of this profile is shown in Figure 4) (1) Bouguer gravity field Δg_B, (2) magnetic field ΔZ, (3) first horizontal derivative of gravity field $\partial \Delta g_B / \partial x$, (4) contour of magnetized body and position of magnetization vector, (5) contour of body determined by analysis of $\partial \Delta g_B / \partial x$

Eastern Mediterranean segment of the Alpine-Himalayan tectonic belt

The Easternmost Mediterranean (EMM) is a tectonically complex region evolving in the long term and located in the midst of the progressive Afro-Eurasian collision within the AHTB (Khain, 1984; Ben-Avraham et al., 2002) (Figure 7). Both rift-oceanic systems and terrane belts are known to have been formed in this collision zone (Stampfli et al., 2013). The formation of its modern complex structure is associated with the evolution of the Neotethys Ocean and its margins (e.g., Ben-Avraham and Ginzburg, 1990; Robertson et al., 1991; Ben-Avraham et al., 2002). The EMM was formed during the initial phase of the Neotethys in the Early and Late Permian (Golonka and Ford, 2000; Stampfli et al., 2013).

The EMM region has attracted increasing attention in connection with the recent discoveries of significant hydrocarbon deposits in this region (Eppelbaum and Katz, 2011; Eppelbaum et al., 2012). Currently seismic prospecting is the main tool used in hydrocarbon deposit discovery. However, even sophisticated seismic data analysis (e.g., Roberts and Peace, 2007; Gardosh et al., 2010; Marlow et al., 2011), fails to identify the full complex structural-tectonic mosaic of this region, and more importantly, is unable to clarify its complex tectonic evolution. This highlights the need for combined analysis of geophysical (first of all, magnetic and gravity (Eppelbaum, 2006)) data associated with the paleomagnetic and paleobiogeographic conditions that can yield deep paleotectonic criteria for unmasking the complex geodynamic pattern of this region (Eppelbaum and Katz, 2015a).

Ben-Avraham et al. (2002) have proved an existence of oceanic crust in the Levant Basin (in the middle of EMM) and continental crust under the Eratosthenes Seamount on the basis of integrated seismic-gravity-magnetic (with thermal data utilization) analysis. Extensive geological-geophysical investigations have been carried out in this region, and a significant number of deep boreholes have been drilled (Eppelbaum and Katz, 2011; 2014b). Geophysical-geological evolution of the EMM in terms of the modern geodynamics (first of all, plate tectonics) is reflected in (Ben-Avraham and Ginzburg, 1990; Ben-Avraham et al., 2002, 2006; Robertson et al., 1998; Jimenez-Munt et al., 2006; Le Pichon and Kreemer, 2010). Integrated geological-geophysical zonation of the deep structure of this region was triggered in (Eppelbaum and Katz, 2011; Eppelbaum and Katz, 2012, 2014b; Eppelbaum et al., 2012, 2014b).

Results of 3D combined gravity-magnetic modeling

Let's consider a few fragments of the carried combined research. The first Moho map of the EMM was constructed on the basis of gravity and seismic data analysis with application of some tectonic-geodynamic reconstructions (Eppelbaum and Pilchin, 2006; Eppelbaum et al., 2012). The first Curie map of Israel (Eppelbaum et al., 2014a) (developed with utilization of thermal, seismic and gravity data and with 3D magnetic modeling) also correlates with the position of the terranes (e.g., Ben-Avraham et al., 2006). The sources of the two most significant gravity-magnetic anomalies in Israel – Hebron and Carmel – were classified (on the basis of 3D gravity-magnetic fields modeling) as phenomena associated with tectonically weakened zones between the terranes (Eppelbaum et al., 2005, 2006).

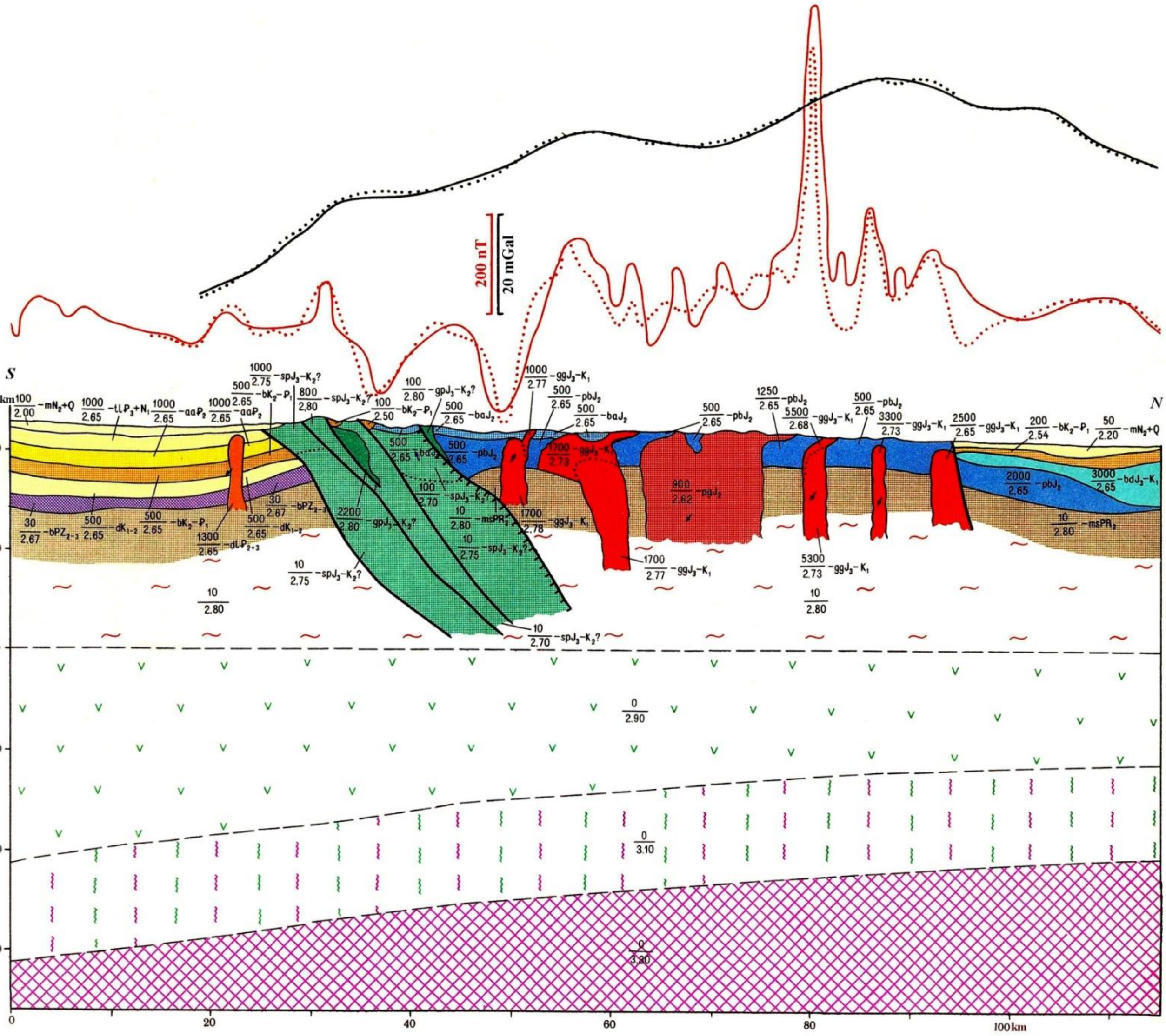

Figure 6. Physical-geological model along Profile 1: Mez-Mazra – Gedabey - Dzegam-Djirdakhan (location of the profile is shown in Figure 4) (after Eppelbaum and Khesin, 2011)

Captions for Figure 6

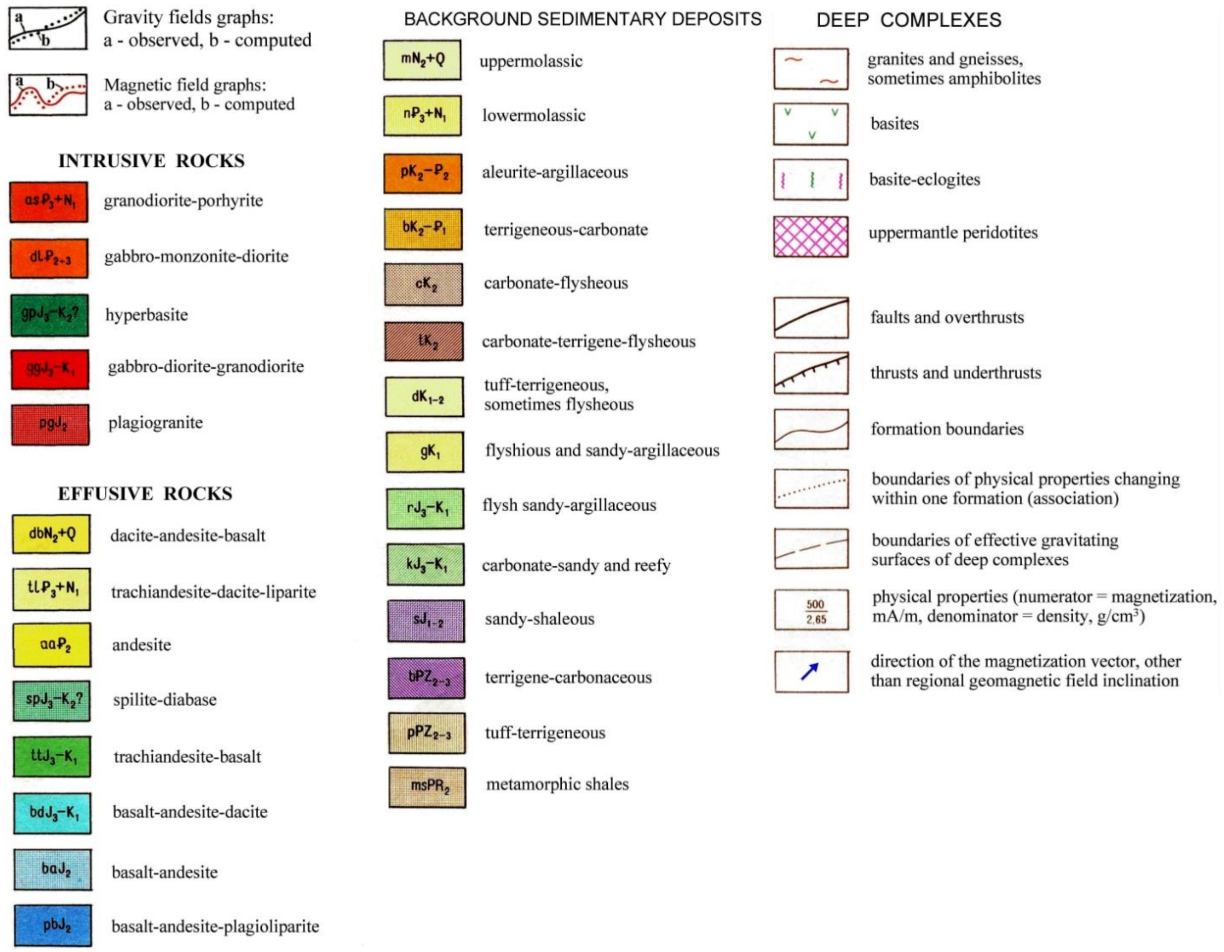

Studying the EMM deep structure demands a careful attention to the blocks of oceanic (basaltic) crust with reverse magnetization that were discovered (Ben-Avraham et al., 2002; Eppelbaum, 2006). This issue was very briefly explained as paleomagnetic Kiama zone of inverse polarity (Eppelbaum and Katz, 2012) and a rather more detailed description was given in (Eppelbaum et al., 2014b; Eppelbaum and Katz, 2015a, 2015b), which demands separate consideration. 3D magnetic analysis conducted along three interpretation profiles supported by gravity-seismic examination along the same lines (location of profiles is shown in Figure 8A) unambiguously indicates the presence of blocks of the Earth's crust with reverse magnetization (Ben-Avraham et al., 2002). By other words, in the mentioned research for a first time combined seismo-magnetic-gravity models for three crossing profiles (Profiles II – II and III – III are shown in Figures 8B and 9, respectively) were developed. It should be noted that the most difficult process was the 3D magnetic field modeling (hundreds of iterations were applied) taking into account very complex and magnetically variable media and requiring the necessity to create a common 3D geometrical model for three geophysical fields. Integrated interpretation of three independent geophysical fields (assuming that each field is characterized by three anomalous points) increases the reliability of interpretation by the use of error function in three times (Eppelbaum, 2014a). In our case the number of anomalous points is many times larger, consequently the reliability of interpretation is greater.

Results of 3D combined magnetic-gravity modeling along Profile I – I are presented in Figure 9. It is obvious that in this ***PGM*** magnetic field modeling is much more complex problem than gravity field modeling. The main peculiarities of this ***PGM*** are discovered crystal block of oceanic crust with inverse magnetization (about -120°) in the center of profile (Ben-Avraham et al., 2002) (faintly yellow colored) and a crystal block of continental crust with inverse magnetization in the eastern part of this profile (about -45°) (brightly yellow colored). A reconstruction of the position of a reverse magnetized block of the Earth's crust enabled us to obtain a magnetization zone with a S – N orientation with a width reaching 70 km and length of about 200 km (Eppelbaum et al., 2014b; Eppelbaum and Katz, 2015a). Such a large, thick (about 10 km) zone (the total volume of this zone exceeds 120,000 km^3) of inverse magnetization must correspond to a significant and prolonged effect of inverse polarity in the Earth's magnetic field history. The Early Cretaceous or Early Jurassic, as was supposed in (Ben-Avraham et al., 2002), do not contain sufficiently prolonged periods of the Earth's magnetic field inverse polarity (Figure 10). It was suggested that this is the Kiama zone of inverse polarity (Eppelbaum et al., 2014b; Eppelbaum and Katz, 2014a) with duration of about 50 mln years (see Figure 10) that was first detected in the Late Carboniferous and Permian in Australia (Irving, 1966).

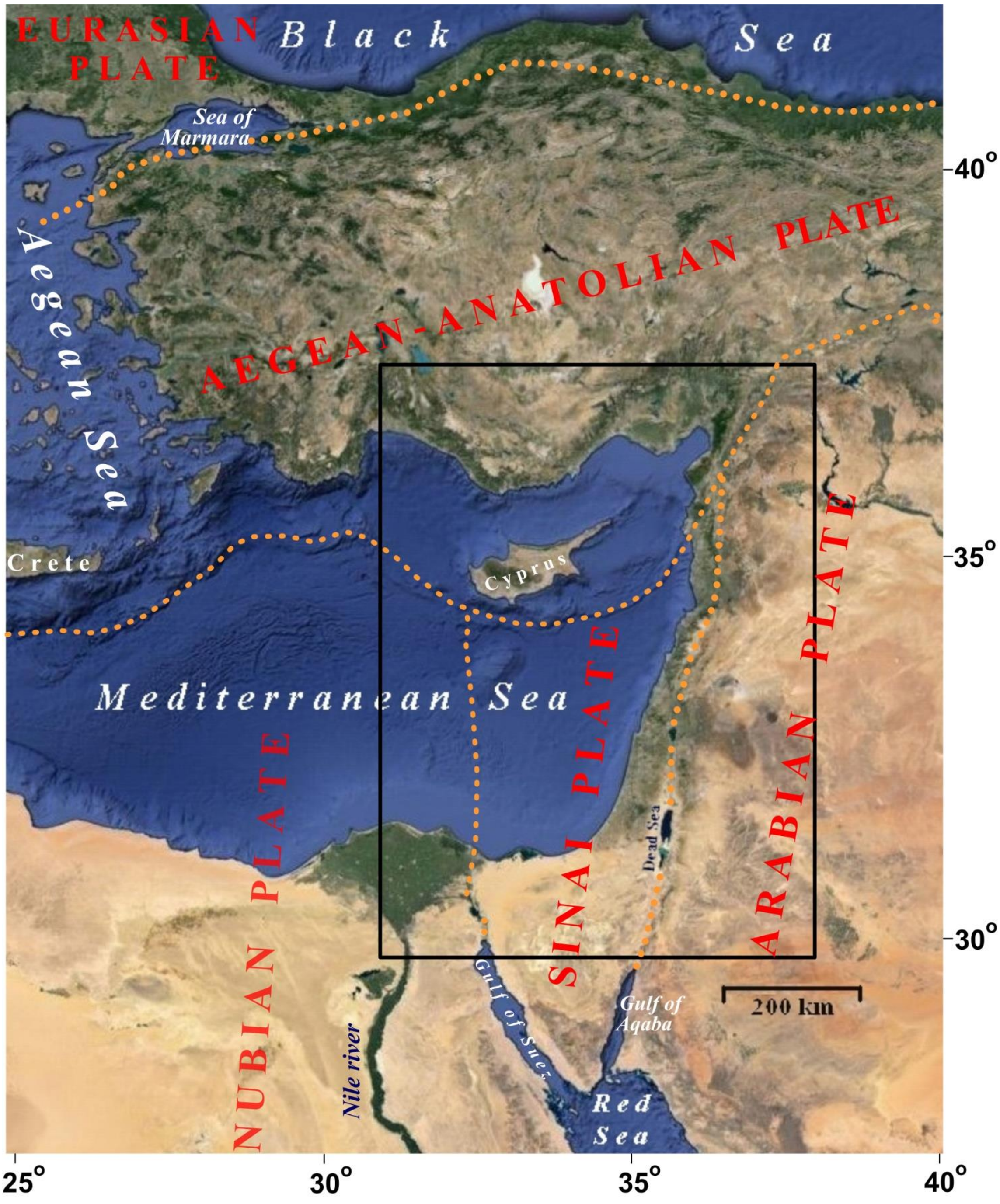

Figure 7. Overview map of the region. The study area is outlined by a black rectangle. Orange dot lines indicate boundaries between tectonic plates

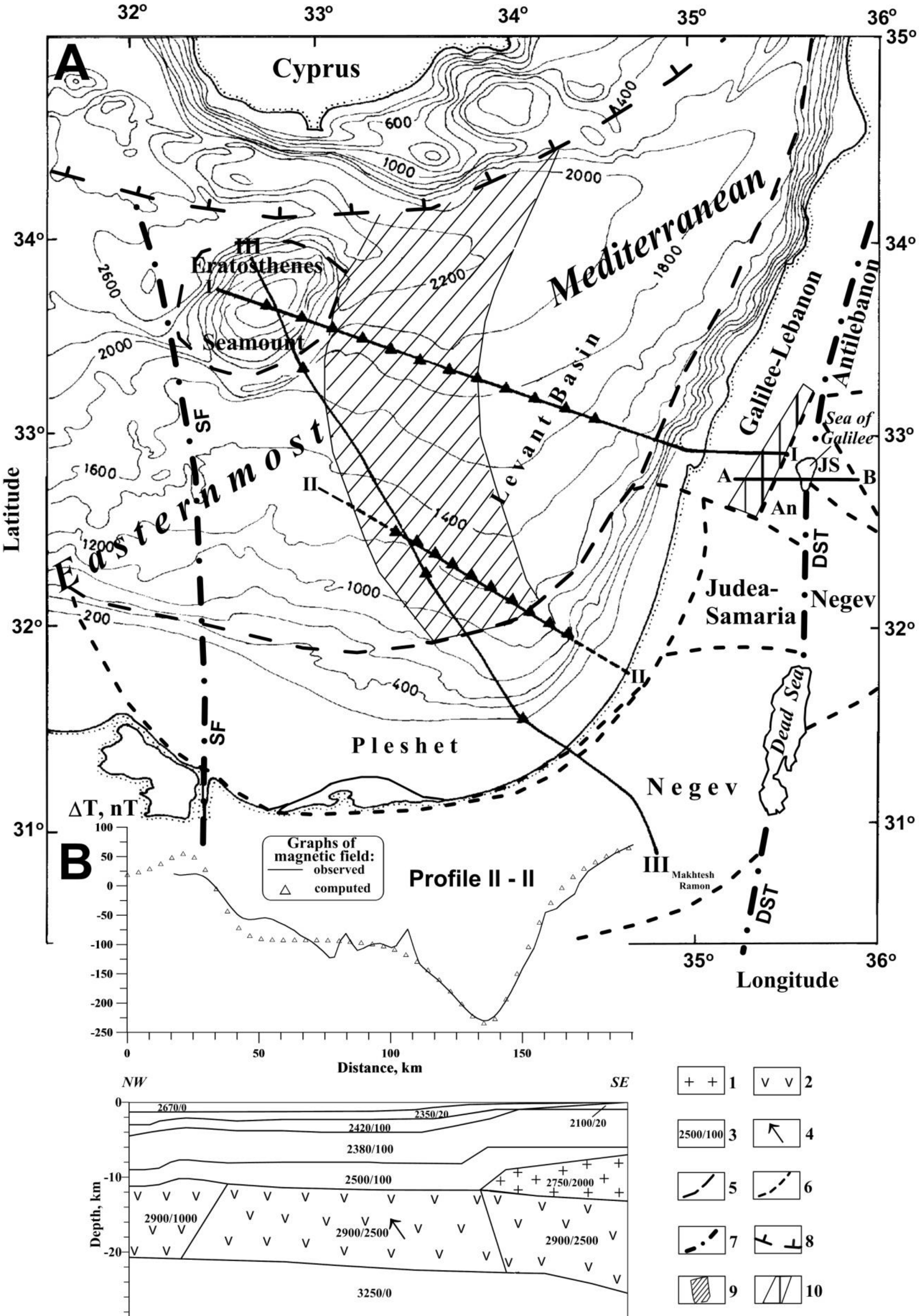

Figure 8. A: Tectono-paleomagnetic map of the region with location of seismic-gravity-magnetic profiles, B: Results of 3D magnetic field modeling along profile II – II

(1) granitic layer, (2) basaltic layer, (3) physical properties (numerator=density, kg/m^3, denominator=magnetization, mA/m), (4) direction of the magnetization vector other than the geomagnetic field inclination of the region, (5) boundary discovered between the continental and oceanic crust within the Sinai plate, (6) faults limiting terrane location, (7) interplate deep faults of the Eastern Mediterranean: SF, Sinai Fault and DST, Dead Sea Transform, (8) deep fault separating the Alpine Belt and oceanic depression of the Easternmost Mediterranean, delineated paleomagnetic zones of inverse polarity: (9) Kiama, (10) Neoproterozoic. JS, Judea-Samaria, An, Antilebanon. (1-5) generalized after Ben-Avraham et al. (2002).

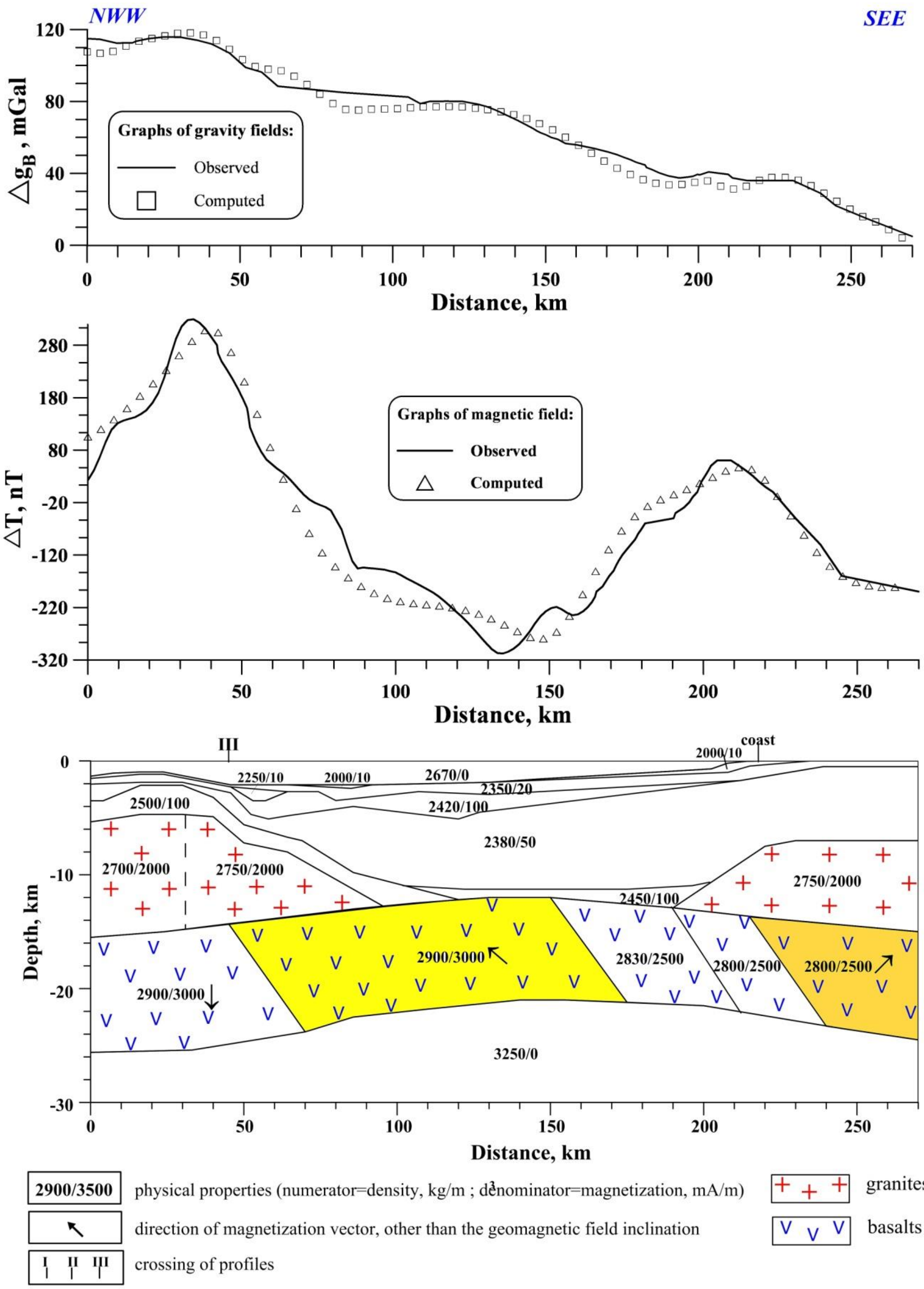

Figure 9. Combined ***PGM*** constructed on the basis of seismic analysis and 3D gravity-magnetic modeling along Profile I – I (location of Profile I – I is shown in Figure 8) (modified after Ben-Avraham et al., 2002)

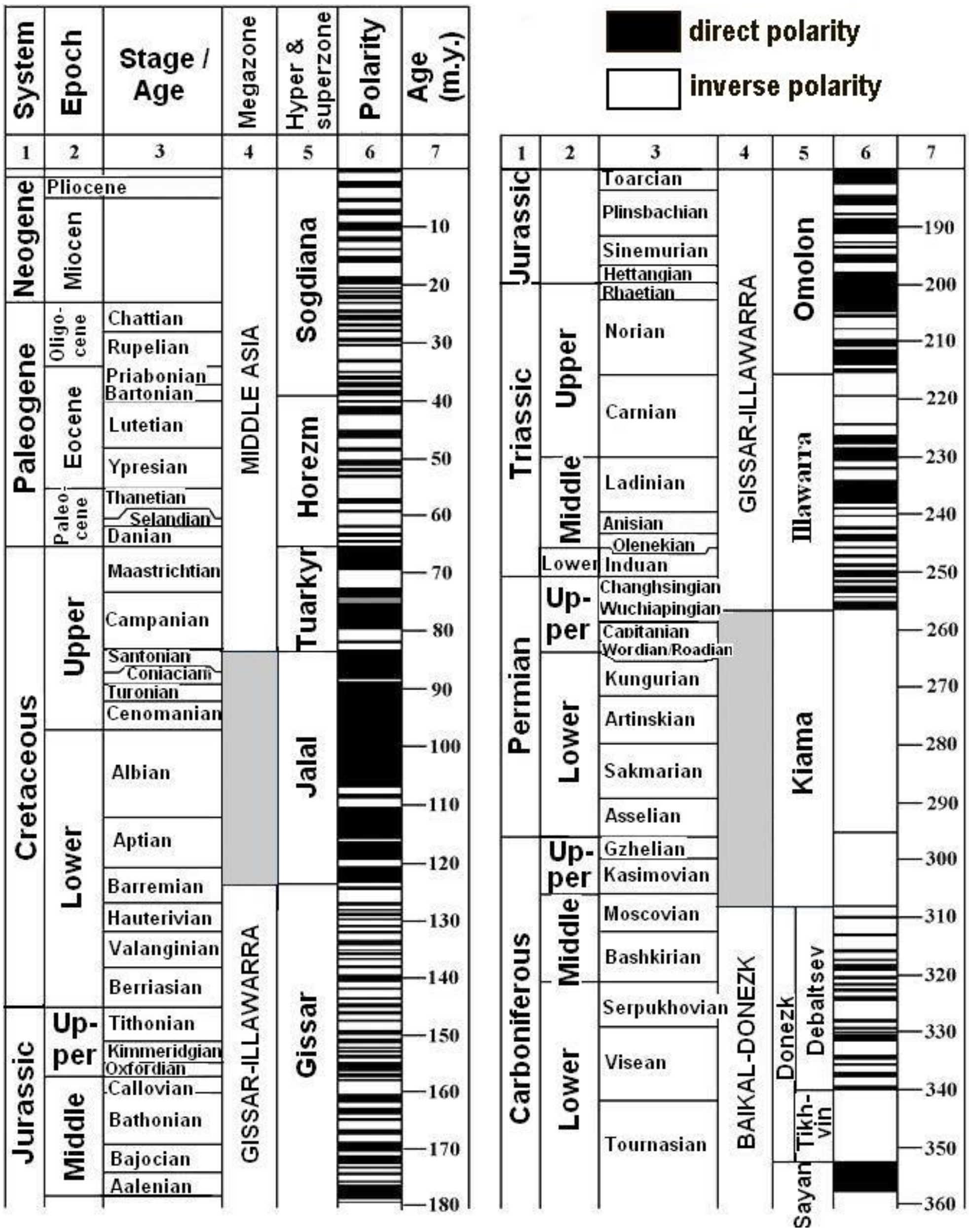

Figure 10. The combined Paleomagnetic Scale – Chronostratigraphic Chart of the most part of the Phanerozoic (compiled on the basis of Molostovsky et al. (1998) and Molostovsky et al. (2007) and Molostovsky (2009) paleomagnetic reconstructions and International Chronostratigraphic Chart (International Commission on Stratigraphy, 2014)

Another example displays the final ***PGM*** along profile crossing the Dead Sea Transform (DST) within the Sea of Galilee (Profile A – B) obtained by use of 3D combined gravity-magnetic field modeling (Figure 11) (location of this profile is presented in Figure 8A). A preliminary ***PGM*** of this profile was constructed on the basis of Rotstein and Bartov (1989), Rotstein et al. (1992), Ben-Avraham et al. (1996), Eppelbaum and Pilchin (2006), Eppelbaum et al. (2007), Meiler et al. (2011), Ben-Avraham et al. (2014).

Negative gravity anomaly along Profile A – B (Figure 11) is caused mainly by the low dense sedimentary deposits and salt accumulated in the DST zone. At the same time comprehensive analysis of magnetic field behavior indicates that it cannot be explained by subsurface basalts effects (and by effects from any basaltic plates occurring at low depth). Such a behavior may provide in these physical-geological conditions only a deep crystal block with an inverse magnetization. A similar crystal block with the same direction of magnetization was

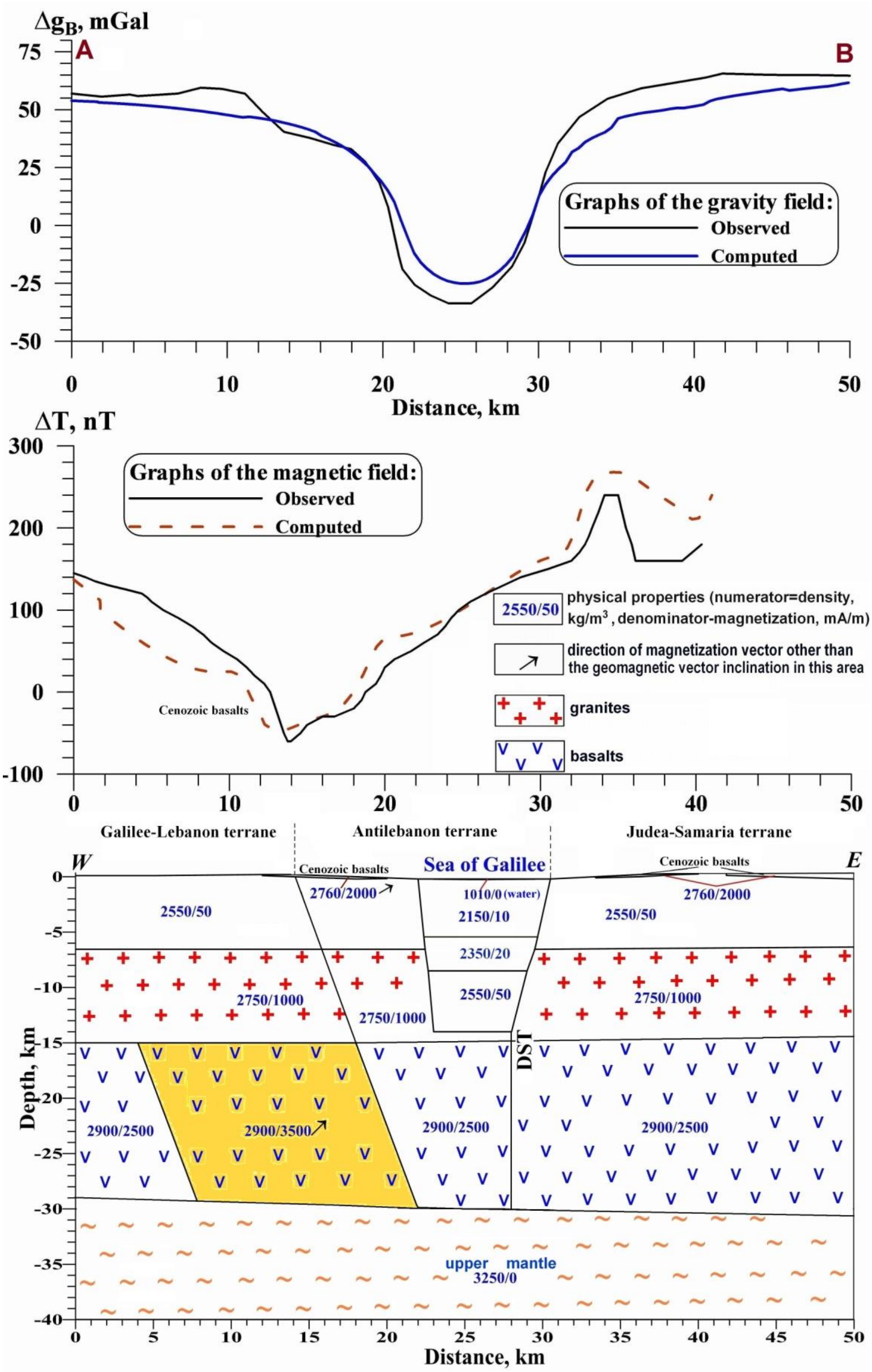

Figure 11. Combined ***PGM*** constructed on the basis of 3D gravity-magnetic modeling and seismic data analysis along profile A – B (location of profile A – B is shown in Figure 8)

discovered in the eastern part of Profile I – I (see Figure 9). Petrographic and radiometric analyses of the Sinai and Arabian shields (see Figure 7) indicate that here occur various complexes of Middle and Upper Precambrian among which dominate Neoproterozoic associations with a radiometric age of 600 – 1000 Ma (e.g., Stern et al., 2004; Johnston and Kattan, 2008). Numerous paleomagnetic examinations of Neoproterozoic display that in these rocks an inverse magnetization is prevailing (Gurevich, 1981; Molostovsky et al., 1998). A generalized paleomagnetic scale of Neoproterozoic (reconstructed by Y. Katz on the basis of numerous paleomagnetic determinations analysis) is presented in Figure 12. Simple visual analysis of this scale indicates that the most intervals of magnetic field inverse polarization relate to 605 – 815 Ma. Thus, we can relate the discovered zone of inverse magnetization (on the basis of Profile I – I (Figure 9) and Profile A – B (Figure 11)) (see the brightly yellow colored blocks) to Neoproterozoic (interval about 210 My, between 605 and 815 Ma). The delineated Neoproterozoic paleomagnetic zone of inverse polarity is contoured in Figure 8A.

Undoubtedly, application of different transformation procedures (upward and downward continuation, calculation of difference anomalies, wavelet, entropy, self-adjusting filtering, etc.) may help to obtain some additional parameters of geological sections which may be useful for 3D gravity-magnetic modeling and ***PGMs*** development. For instance, recently developed new integrated wavelet approaches (e.g., Eppelbaum et al., 2011) enable to join results of geophysical methods based on different physical principles (for instance, magnetics and seismics). However, presentation of such examples is beyond of the goal of this article.

It should be noted that for solving different tectonic and geodynamic problems both in the South Caucasus and EMM can be effectively applied the satellite observed gravity and magnetic data (measured with the same grid and accuracy and having an important property of repetition). A successful example of the tectono-geodynamic examination of satellite derived gravity data for the EMM was demonstrated in Eppelbaum and Katz (2015b). Exploration of satellite observed magnetic data for studying deep structure in the considered above scale is more complex problem. For this aim, apparently, complex Gaussian function and advanced wavelet transform (i.e., Alperovich et al., 2013) may be employed.

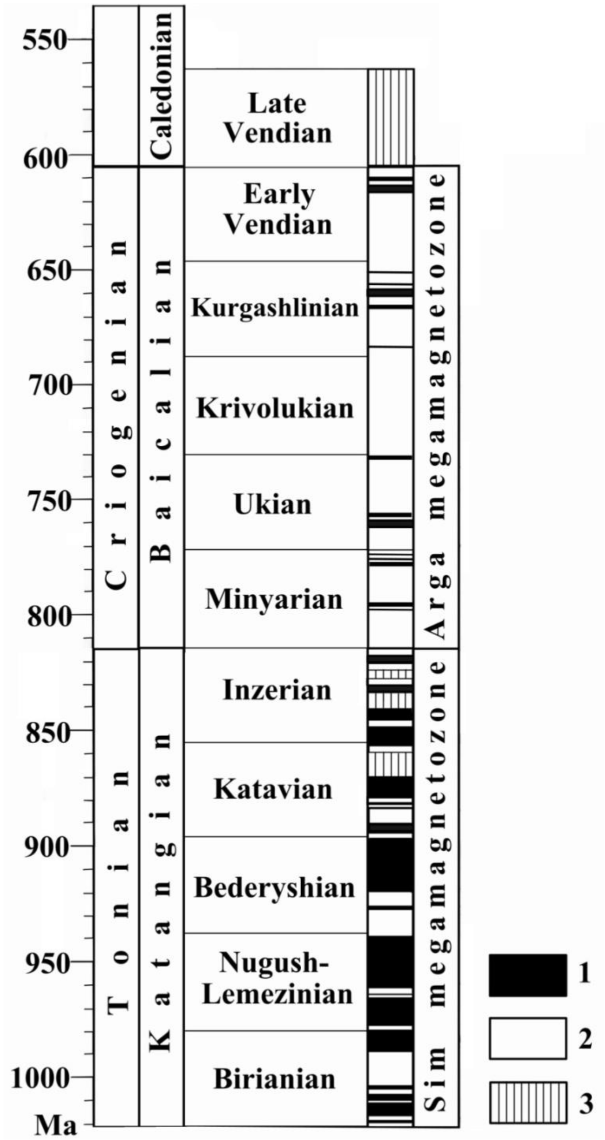

Figure 12. A generalized paleomagnetic scale of Neoproterozoic (complied by Y. Katz, Tel Aviv University).
(1) direct polarity, (2) inverse polarity, (3) alternating polarity

Comparison of results of 3D combined gravity-magnetic field modeling in the South Caucasus and EMM indicate that in both regions characterized by different tectono-structural and other peculiarities the skillful modeling may provide important results that can be used for construction of geodynamic models, searching economic deposits and long-term seismological prognosis.

Conclusions

It can be concluded that 3D combined gravity-magnetic field modeling is a powerful interpretation tool for recognizing deep structure of complex geological regions. Application of this methodology together with petrophysical and paleomagnetic examination, seismic, magnetotulliric, thermal and other investigations allowed to unmasking deep geological structure of such complex regions as the South Caucasian and Easternmost Mediterranean segments of the Alpine-Himalayan tectonic belt. The process of 3D modeling, taking into account a constant necessity of interrelation between the physical, mathematical, tectonic, structural and some other factors, supposes a high qualification level of the interpreter (interpreters). A further evolution of this methodology will consist not only in analysis and application of modern tectonic-geodynamic conceptions, but and in wide attraction and of different geological-geophysical data, including comprehensive utilization of satellite observed (constantly renewing) gravity and magnetic arrays.

Acknowledgements

Author would like to thank Prof., Academician of the Georgian Acad. of Sci. T. Chelidze and Dr. S. Gongadze as well as anonymous reviewers, who thoroughly reviewed the manuscript, and whose critical comments and valuable suggestions were very helpful in preparing this paper. The research leading to these results has received funding from the Ministry of Energy, National Infrastructures and Water Resources of Israel under Grant Agreement No. 212-17-018.

REFERENCES

ALEXEYEV, V.V., GADJIEV, T.G., KARKOSHKIN, A.I., KHESIN, B.E., ISMAIL-ZADEH, T.A. 1988. Gravity and magnetic anomalies in Azerbaijan and their geological interpretation. Map Printing Factory. Leningrad (in Russian).

ALEXIDZE, M.A., GUGUNAVA, G.E., KIRIA, D.K., CHELIDZE, T.L. 1993. A three-dimensional stationary model of the thermal and thermoelastic fields of the Caucasus. *Tectonophysics*, **227**, 191-203.

ALLEN, M.B., VINCENT, S.J., ALSOP, G.I., ISMAIL-ZADEH, A., FLECKER, R. 2003. Late Cenozoic deformation in the South Caspian region: effects of a rigid basement block within a collision zone. *Tectonophysics*, **366**, 223-239.

ALIZADEH, AK.A. (Ed.). 2005. Geology of Azerbaijan. Vol. **5**: Physics of the Earth. Nafta Press. Baku (in Russian).

ALI-ZADEH, AK.A. (Ed.). 2012. Modern problems of geology and geophysics of the Caucasus. Nafta Press. Baku.

ALPEROVICH, L., EPPELBAUM, L., ZHELUDEV, V., DUMOULIN, J., SOLDOVIERI, F., PROTO, M., BAVUSI, M., LOPERTE, A. 2013. A new combined wavelet methodology applied to GPR and ERT data in the Montagnole experiment (French Alps). *Journal of Geophysics and Engineering*, **10**, 2, 025017, 1-17.

AZIZBEKOV, SH.A., AGABEKOV, M.G., GRIGORYANTS, B.V., SHIKALIBEYLI, E.SH., MAMEDOV, A.V. 1972. The history of the geological evolution. In: Azizbekov Sh.A. (Ed.), *Geology of the USSR, Azerbaijan*, Vol. **XLVII**, Nedra, Moscow, 441-503 (in Russian).

ARTYUSHKOV, E.V., MÖRNER, N.-A., TARLING, D.H. 2000. The cause of loss of lithospheric rigidity in areas far from plate tectonic activity. *Geophysical Jour. International*, **143**, 752-766.

BARTON, P.J. 1986. The relationship between seismic velocity and density in the continental crust – A useful constraint? *Geophys. Jour. Royal. Astr. Soc*., **87**, 195-208.

BEN-AVRAHAM, Z., GINZBURG, A. 1990. Displaced terranes and crustal evolution of the Levant and the eastern Mediterranean. *Tectonics*, **9**, 613-622.

BEN-AVRAHAM, Z., GINZBURG, A., MAKRIS, J., EPPELBAUM, L. 2002. Crustal structure of the Levant basin, eastern Mediterranean. *Tectonophysics*, **346**, 23-43.

BEN-AVRAHAM, Z., ROZENTHAL, M., TIBOR, G., NAVON, H., WUST-BLOCH, H., HOFSTETTER, R., RYBAKOV, M. 2014. Lake Kinneret, ecology and management. In: *Structure and Tectonic Development of the Kinneret Basin* (Ed. T. Zohary et al.), Aquatic Ecology Series, **6**, Springer, 19-38.

BEN-AVRAHAM, Z. SCHATTNER, U., LAZAR, M., HALL, J.K., BEN-GAI, Y., NEEV, D., RESHEF, M. 2006. Segmentation of the Levant continental margin, eastern Mediterranean. *Tectonics*, TC5002, **25**, 1-17.

BEN-AVRAHAM, Z., TEN-BRINK, U., BELL, R., REZNIKOV, M. 1996. Gravity field over the Sea of Galilee: evidence for a composite basin along a transform fault. *Jour. Geophys. Res*earch, **101**, 533-544.

BRUNET, M.-F., KOROTAEV, M.V., ERSHOV A.V., NIKISHIN, A.M. 2003. The South Caspian Basin: a review of its evolution from subsidence modelling. *Sedimentary Geology*, **156**, 119-148.

EPPELBAUM, L.V. 2006. Methodology of 3-D combined modeling of magnetic and gravity fields in the Eastern Mediterranean. *Proceed. of the 3rd EUG Meeting*, Vienna, Austria, **8**, 02057, 1-4.

EPPELBAUM, L.V. 2014a. Four color theorem and applied geophysics. *Applied Mathematics*, **5**, 358-366.

EPPELBAUM, L.V. 2014b. Estimating informational content in geophysical observations on example of searching economic minerals in Azerbaijan. *Izv. Acad. Sci. Azerb. Rep., Earth Sciences*, 3-4, 31-40.

EPPELBAUM, L.V., ALPEROVICH, L., ZHELUDEV, V., PECHERSKY, A. 2011. Application of informational and wavelet approaches for integrated processing of geophysical data in complex environments. *Proceed. of the 2011 SAGEEP Conference*, Charleston, South Carolina, USA, **24**, 24-60.

EPPELBAUM, L., BEN-AVRAHAM, Z., KATZ, Y. 2005. Does mantle diapir produce Hebron magnetic anomaly? *Trans. of the Conf. of the Israel Geol. Soc. Ann. Meet*., Moshabim Country Logging (Negev), Israel, 26 p.

EPPELBAUM, L.V., BEN-AVRAHAM, Z., KATZ, Y.I. 2007. Structure of the Sea of Galilee and Kinarot Valley derived from combined geological-geophysical analysis. *First Break*, **25**, 1, 21-28.

EPPELBAUM, L., KATZ, Y. 2011. Tectonic-Geophysical Mapping of Israel and eastern Mediterranean: Implication for Hydrocarbon Prospecting. *Positioning*, **2,** 1, doi: 10.4236/pos.2011.21004, 36-54.

EPPELBAUM, L.V., KATZ, Y.I. 2012. Key features of seismo-neotectonic pattern of the Eastern Mediterranean. *Proceedings of Azerb. Nat. Acad. of Sci., Earth Sciences*, 3, 29-40.

EPPELBAUM, L.V., KATZ, Y.I. 2014a. First paleomagnetic map of the Easternmost Mediterranean derived from combined geophysical-geological analysis. *Trans. of the 10th EUG Meet., Geophysical Research Abstracts*, **16**, EGU2014-2424, Vienna, Austria, 1-5.

EPPELBAUM, L.V., KATZ, Y.I. 2014b. First maps of Mesozoic and Cenozoic structural-sedimentation floors of the Easternmost Mediterranean and their relationship with the deep geophysical-geological zonation. *Proceed. of the 19th Intern. Congress of Sedimentologists*, Geneva, Switzerland, 1-3.

EPPELBAUM, L.V., KATZ, Y.I. 2015a. Newly developed paleomagnetic map of the Easternmost Mediterranean unmasks geodynamic history of this region. *Central European Jour. of Geosciences*, **7**, 1, 95-117.

EPPELBAUM, L.V., KATZ, Yu.I. 2015b. Eastern Mediterranean: Combined geological-geophysical zonation and paleogeodynamics of the Mesozoic and Cenozoic structural-sedimentation stages. *Marine and Petroleum Geology*, **65**, 198-216.

EPPELBAUM, L., KATZ, Y., BEN-AVRAHAM, Z. 2006. Mt. Carmel structure as a plate tectonics phenomenon. *Trans. of the Conf. of the Israel Geol. Soc., Ann. Meet.*, Beit-Shean, Israel, 31.

EPPELBAUM, L.V., KATZ, Y.I., BEN-AVRAHAM, Z. 2012. Israel – Petroleum Geology and Prospective Provinces. *AAPG European Newsletter*, 4, 4-9.

EPPELBAUM, L.V., KHESIN, B.E. 2004. Advanced 3-D modelling of gravity field unmasks reserves of a pyrite-polymetallic deposit: A case study from the Greater Caucasus. *First Break*, **22**, 11, 53-56.

EPPELBAUM, L.V., KHESIN, B.E. 2012. Geophysical studies in the Caucasus. Springer.

EPPELBAUM, L.V., KUTASOV, I.M., PILCHIN, A.N. 2014a. Applied geothermics. Springer.

EPPELBAUM, L.V., ITKIS, S.E., KHESIN, B.E. 2000. Optimization of magnetic investigations in the archaeological sites in Israel. In Special Issue of Prospezioni Archeologiche*: Filtering, Modeling and Interpretation of Geophysical Fields at Archaeological Objects*, 65-92.

EPPELBAUM, L.V., NIKOLAEV, A.V., KATZ, Y.I. 2014b. Space location of the Kiama paleomagnetic hyperzone of inverse polarity in the crust of the eastern Mediterranean. *Doklady Earth Sciences* (Springer), **457**, 6, 710-714.

EPPELBAUM, L.V., PILCHIN, A.N. 2006. Methodology of Curie discontinuity map development for regions with low thermal characteristics: An example from Israel. *Earth and Planetary Sciences Letters*, **243**, 3-4, 536-551.

ETIRMISHLI, G.D., KAZIMOVA, S.E. 2013. Velocity model of crust of Azerbaijan from the data of digital seismic stations. *Geology and Geophysics of South of Russia*, 1, 59-74.

FORTE, A.M., COWGILL, E., MURTUZAYEV, I., KANGARLI, T., STOICA, M. 2013. Structural geometries and magnitude of shortening in the eastern Kura fold-thrust belt, Azerbaijan: Implications for the development of the Greater Caucasus Mountains. *Tectonics*, **32**, 688-717.

GADJIEV, R.M. 1965. Deep geological structure of Azerbaijan. Azgosizdat. Baku (in Russian).

GAMKRELIDZE, I.R., SHENGELIA, D.M. 2007. Pre-Alpine geodynamics of the Caucasus, suprasubduction regional metamorphism and granitoid magmatism. *Bull. of the Georgian National Acad. of Sci*., **175**, 1, 57-65.

GARDOSH, M.A., GARFUNKEL, Z., DRUCKMAN, Y., BUCHBINDER, B. 2010. Tethyan rifting in the Levant Region and its role in Early Mesozoic crustal evolution. *Geological Society*, London, **341**, 9-36.

GASANOV, A.G. 2001. Deep structure and seismicity of Azerbaijan in relation to hydrocarbons prognosis. Elm. Baku (in Russian).

GOLONKA, J., FORD, D. 2000. Pangean (Late Carboniferous – Middle Jurassic) paleoenvironment and lithofacies. *Palaeogeography, Paleoclimatology, Paleoecology*, **161**, 1-34.

GULIYEV, I., PANAHI, B. 2004. Geodynamics of the deep sedimentary basin the Caspian sea region: paragenetic correlation of the seismicity and mud volcanism. *Geo-Marine Letters*, **24**, 3, 169-176.

GUREVICH, E.L. 1981. Paleomagnetism of Upper Precambrian rocks of Irkutian amphitheatre; Problems of their correlation and paleogeographic location. In: *Paleomagnetism and Problems of Paleogeography, Transactions of VNIGRI*, 11-22 (in Russian).

IRVING, E. 1966. Paleomagnetism of some carboniferous rocks from New South Wales and its relation to geological events. *Jour. of Geophysical Research*, **71**, 24, 6025-6051.

JIMENEZ-MUNT, I., SABADINI, R., GARDI, A. 2006. Active deformation in the Mediterranean from Gibraltar to Anatolia inferred from numerical modeling and geodetic and seismological data. *Jour. of Geophysical Research*, **108**, B1, doi: 10.1029/2001JB001544, 1-24.

JOHNSON, P.R., KATTAN, F.H. 2008. Lithostratigraphic revision in the Arabian shield: The impacts of geochronology and tectonic analysis. *The Arabian Jour. for Science and Engin*., **33**, 1, 3-16.

KADIROV, F.A. 2000. Gravity field and models of deep structure of Azerbaijan. Nafta Press. Baku (in Russian).

KADIROV, F.A. 2006. Nature of gravitational anomaly in the South Caspian Basin. *Trans. of the EAGE 68th Conference*, Vienna, P325, 1-4.

KADIROV, F.A., GADIROV, A.H. 2014. A gravity model of the deep structure of South Caspian Basin along submeridional profile Alborz–Absheron Sill. *Global and Planetary Change*, **114**, 66-74.

KABAN, M.K. 2002. A gravity model of the north Eurasia crust and upper mantle: 2. The Alpine-Mediterranean fold belt and adjacent structures of the southern former USSR. *Russian Journal of Earth Sci*., **4**, 1, 19-33.

KHAIN, V.E. 1975. Structure and main stages in the tectonic-magmatic development of the Caucasus: An attempt at geodynamic interpretation. *American Jour. of Science*. **275A**, 131-156.

KHAIN, V.E. 1984. Regional geodynamics. Alpine Mediterranean Belt. Nedra. Moscow (in Russian).

KHAIN, V.E. 2000. Tectonics of continents and oceans. Nauchnyi Mir. Moscow (in Russian).

KHAIN V.E. 2007. Mesozoic–Cenozoic Accretionary complexes of the Greater Caucasus. *Doklady Earth Sciences*, **413A**, 3, 376-379.

KHAIN, V.E., ALIZADEH, AK.A. (Eds.). 2005. Geology of Azerbaijan. Vol. 4: Tectonics. Nafta Press. Baku (in Russian).

KHALAFLY, A.A. 2006. Paleomagnetism and some problems of shear deformations of the Lesser Caucasus. Takhsil. Baku (in Russian).

KHESIN, B.E., ALEXEYEV, V.V., EPPELBAUM, L.V. 1993. 3-D modelling of gravity and magnetic fields as a final stage of application of effective interpretation system of geophysical data under difficult geological conditions. *Geoinformatics*, **4**, 3, 177-188.

KHESIN, B.E., ALEXEYEV, V.V., EPPELBAUM, L.V. 1996. Interpretation of geophysical fields in complicated environments. Kluwer Academic Publisher (Springer). Ser: Modern Approaches in Geophysics. Boston – Dordrecht – London.

KOULAKOV, I., ZABELINA, I., AMANATASHVILI, I., MESHKINA, V. 2012. Nature of orogenesis and volcanism in the Caucasus region based on results of regional tomography. *Solid Earth*, **3**, 327-337.

LE PICHON, X., KREEMER, C. 2010. The Miocene-to-present kinematic evolution of the Eastern Mediterranean and Middle East and its implications for dynamics. *Annu. Rev. Earth Planet. Sci*., **38**, 323-351.

LEONOV, Yu.G. (Ed.), 2008. The Greater Caucasus in the Alpine Epoch. Geos. Moscow (in Russian).

MARLOW, L., KORNPIHL, K., KENDALL, C.G.ST.C. 2011. 2-D basin modeling study of petroleum systems in the Levantine Basin, Eastern Mediterranean. *Geoarabia*, **16**, 2, 17-42.

MAMEDOV, P.Z. 2009. Sedimentation models in the SCMB and their seismostratigraphic characteristics. *Stratigraphy and Sedimentology of Oil-Gas Basins*, 3, 70-85.

MEDERER, J., MORITZ R., ULIANOV A., CHIARADIA, M. 2013. Middle Jurassic to Cenozoic evolution of arc magmatism during Neotethys subduction and arc-continent collision in the Kapan Zone, southern Armenia. *Lithos*, **177**, 61-78.

MEILER, M., RESHEF, M., SHULMAN, H. 2011. Seismic depth-domain stratigraphic classification of the Golan Heights, central Dead Sea Fault. *Tectonophysics*, **510**, 354-369.

MOLOSTOVSKY, E.A., MOLOSTOVSKY, I.I., MINIKH, M.G. 1998. Stratigraphic correlations of the Upper Permian and Triassic beds from the Volga-Ural and Cis-Caspian. In: (Crasquin-Soleau, S. and Barrier, E´., Eds.) *Peri-Tethys memoir 3: Stratigraphy and Evolution of Peri-Tethyan platforms*. *Me´moires du Muse´um national d'histoire naturelle*, Paris, **177**, 35-44.

MOLOSTOVSKY, E.A., PECHERSKY, D.M., FROLOV, I.Yu. 2007. Magnetostratigraphic timescale of the Phanerozoic and its description using a cumulative distribution function. *Izvestiya, Physics of the Solid Earth*, **43**, 10, 811-818.

MOLOSTOVSKY, E.A. 2009. An improved magnetostratigraphic scale of Phanerozoic. *A report prepared for the Russ. Acad. of Sci*. (in Russian).

MOSAR, J., KANGARLI, T., BOCHUD, M., GLASMACHER, U.A., RAST, A., BRUNET M.-F., SOSSON, M. 2010. Cenozoic–Recent tectonics and uplift in the Greater Caucasus: A perspective from Azerbaijan. *Geological Society*, London, *Special Publications*, 340, 261-280.

MUMLADZE, T., FORTE, A.M., COWGILL, E.S., TREXLER, C.C., NIEMI, N.A., YIKILMAZ, M.B., KELLOGG, L.H. 2015. Subducted, detached, and torn slabs beneath the Greater Caucasus. *Geores J.*, **5**, 36-46.

PAVLENKOVA, G.A. 2012. Structure of the Caucasus' earth crust along the deep seismic sounding profiles Stepnoe-Bakuriani and Volgograd-Nakhchevan (results of initial data re-interpretation). *Izvestiya, Physics of the Earth*, 5, 16-25.

PILCHIN, A.N., EPPELBAUM, L.V. 1997. Determination of magnetized bodies lower edges by using geothermal data. *Geophysical Journal International*, **128**, 1, 167-174.

RAPPEL, C., McNUTT, M. 1990. Regional compensation of the Greater Caucasus mountains based on an analysis of Bouguer gravity data. *Earth and Planetary Science Letters*, **98**, 360-379.

REILINGER, R., McCLUSKY, S., VERNANT, P. LAWRENCE, S., ERGINTAV, S., CAKMAK, R., OZENER, H., KADIROV, F., GULIEV, I., STEPANYAN, R., NADARIYA, M., HAHUBIA, G., MAHMOUD, S., SAKR, K., ARRAJEHI, A., PARADISSIS, D., AL-AYDRUS, A., PRILEPIN, M., GUSEVA, T., EVREN, E., DMITROTSA, A., FILIKOV, V., GOMEZ, F., AL-GHAZZI, R., KARAM, G. 2006. GPS constraints on continental deformation in the Africa-Arabia-Eurasia continental collision zone and implications for the dynamics of plate interactions. *Jour. of Geophysical Research,* **111**, B05411, 1-26.

RICKETTS, J.W., TAKEDATSU, R., MELLORS, R.J., SANDWELL, D., GOK, R., YETIRMISHLI, G. 2008. Crustal structure of the Caucasus and Caspian Region using gravity and receiver functions. *Proceed. of the American Geophysical Union Fall Meet*., abstract #T21A-1922.

RIORDAN, J. 2014. An Introduction to Combinatorial Analysis. Princeton Univ. Press.

ROBERTS, G., PEACE, D. 2007. Hydrocarbon plays and prospectivity of the Levantine Basin, offshore Lebanon and Syria from modern seismic data. *GeoArabia*, **12**, 3, 99-124.

ROBERTSON, A.H.F., CLIFT, P.D., DEGNAN, P.J., JONES, G. 1991. Palaeogeographic and palaeotectonic evolution of the Eastern Mediterranean Neotethys. *Palaeogeography, Palaeoclimatology, Palaeoecology*, **87**, 289-343.

ROTSTEIN, Y., BARTOV, Y. 1989. Seismic reflection across a continental transform: An example from a convergent segment of the Dead Sea rift. *Jour. of Geophys. Research,* **94**, 2902-2912.

ROTSTEIN, Y., BARTOV, Y., FREISLANDER, U. 1992. Evidence for local shifting of the main fault and changes in the structural setting, Kinarot basin, Dead Sea transform. *Geology*, **20**, 251-254.

RUBAN, D.A. 2013. The Greater Caucasus – A Galatian or Hanseatic terrane? Comment on "The formation of Pangea" by G.M. Stampfli, C. Hochard, C. Vérard, C.Wilhem and J. von Raumer [*Tectonophysics*, **593** (2013), 1-19]. *Tectonophysics*, **608**, 1442-1444.

SAINTOT, A., BRUNET, M.-F., YAKOVLEV, F., SEBRIER, M., STEPHENSON, R., ERSHOV, A., CHALOT-PRAT, F., MCCANN, T. 2006. The Mesozoic-Cenozoic tectonic evolution of the Greater Caucasus. *The Geological Society of London*, Memoirs, **32**, 277-289.

SARKER, G., ABERS, G.A. 1998. Deep structures along the boundary of a collision belt: attenuation tomography of P and S waves in the Greater Caucasus. *Geophysical Jour. International*, **133**, 326-340.

SHARKOV, E., LEBEDEV, V., CHUGAEV, A., ZABARINSKAYA, L., RODNIKOV, A., SERGEEVA, N., SAFONOVA, I. 2015. The Caucasian-Arabian segment of the Alpine-Himalayan collisional belt: Geology, volcanism and neotectonics. *Geosciences Frontiers*, Vol. **6**, No. 4, pp. 513-522.

SHEKINSKY, E., RADZHABOV, M., TIMUKYAN, G., LEVI, V., RIGER, R. 1967. Study of the Earth's crust structure in Azerbaijan using deep seismic sounding. *Izv. Akad. Nauk Azerb. SSR*, Nauki o Zemle, 5, 41-50 (in Russian).

SHIKHALIBEYLI, E.SH. 1972. Location of Azerbaijan in general structure of the Caucasus and surrounding folded region, In: AZIZBEKOV, SH.A. (Ed.), Geology of the USSR, Azerbaijan, Vol. XLVII. Nedra, Moscow, 286-290 (in Russian).

SPICHAK, V.V. 2006. Comparative analysis of hypotheses of the geoelectric structure of the Transcaucasian region from magnetotelluric data. *Izvestiya, Physics of the Solid Earth*, **42**, 1, 60-68.

STAMPFLI, G.M., HOCHARD, C., VÉRARD, C., WILHEM, C., VON RAUMER, J. 2013. The formation of Pangea. *Tectonophysics*, **593**, 1-19.

STERN, R.J., JOHNSON, P.R., KRONER, A., YIBAS, B. 2004. Neoproterozoic ophiolites of the Arabian-Nubian shield. *Developments of in Precambrian Geology*, **13**, 95-128.

STRAKHOV, V.N. 1976. Main ideas and methods for deriving information from gravitational and magnetic observations. Nedra. Moscow (in Russian).

TZIMELZON, I.O. 1965. Deep structure of the Earth's crust and tectonics of Azerbaijan on the geophysical data analysis. *Soviet Geology*, 4, 103-111 (in Russian).

TZIMELZON, I.O. 1970. Relation between the tectonics of sedimentary deposits of Azerbaijan and earth's deep structure. *Geotectonics*, 5, 69-81 (in Russian).